JACS
JOURNAL OF THE AMERICAN CHEMICAL SOCIETY
Communication
pubs.acs.org/JACS

Highly Strained Iron(II) Polypyridines: Exploiting the Quintet Manifold To Extend the Lifetime of MLCT Excited States

Samuel G. Shepard,[†,‡] Steven M. Fatur,[†,‡] Anthony K. Rappé,[§] and Niels H. Damrauer*[,†]

[†]Department of Chemistry and Biochemistry, University of Colorado Boulder, Boulder, Colorado 80309, United States
[§]Department of Chemistry, Colorado State University, Fort Collins, Colorado 80523, United States

Supporting Information

ABSTRACT: Halogen substitution at the 6 and 6″ positions of terpyridine (6,6″-Cl_2-2,2:6′,2″-terpyridine = dctpy) is used to produce a room-temperature high-spin iron(II) complex $[Fe(dctpy)_2](BF_4)_2$. Using UV−vis absorption, spectroelectrochemistry, transient absorption, and TD-DFT calculations, we present evidence that the quintet metal-to-ligand charge-transfer excited state (^{5}MLCT) can be accessed via visible light absorption and that the thermalized ^{5,7}MLCT is long-lived at 16 ps, representing a > 100 fold increase compared to the ^{1,3}MLCT within species such as $[Fe(bpy)_3]^{2+}$. This result opens a new strategy for extending iron(II) MLCT lifetimes for potential use in photoredox processes.

Controlling nonradiative relaxation pathways is an essential component in the design of molecular systems that engage in the conversion of light to chemical or electrical potential. Ruthenium(II) polypyridyl complexes, and in particular 2,2′-bipyridine (bpy) derivatives, have found broad use in applications tied to solar energy conversion[1,2] as well as the burgeoning field of photoredox catalysis.[3−5] This utility is due to the energetic ordering of metal-to-ligand charge-transfer (MLCT) excited states below ligand field (LF) excited states whose structural perturbations, via population of metal−ligand antibonding orbitals, provide facile pathways for energy loss. Iron(II) polypyridyl complexes, on the other hand, have lower energy LF excited states due to a decrease in metal−ligand covalency. With these in play, MLCT deactivation is extremely rapid.[6−10] Whereas the ^{3}MLCT of $[Ru(bpy)_3]^{2+}$ survives for ∼1 μs in room-temperature fluid solution, the ^{1,3}MLCT manifold in $[Fe(bpy)_3]^{2+}$ is lost to a ^{3}LF state in 150 fs, according to recent x-ray fluorescence measurements.[8] That state is further deactivated to a lower energy ^{5}LF state (∼25% of the ^{1}MLCT energy) in 50 fs.[8] Alternatively, recent transient absorption (TA) experiments argue that the ^{5}LF state is impulsively populated in <50 fs.[10] In light of these dynamics, iron(II) polypyridyl systems have been recognized as useful platforms to explore ultrafast structural rearrangements[9,11−13] as well as in applications involving the control of spin.[14,15]

Recent efforts to extend MLCT lifetimes in Fe(II) systems, primarily for purposes of solar energy conversion, have focused on structural modifications that aim to increase the LF.[16−20] For example, McCusker et al. have explored expanded tridentate ligands, bis-complexes of which better approach an octahedral field than the standard 2,2′:6′,2″-terpyridine (tpy) or substituted derivatives.[16] While it is argued that a LF is reached such that the $^5T_2$ and $^3T_1$ excited states switch their energetic ordering (a phenomenon that is rare), the deactivation of the MLCT remains ultrafast. In a different approach, Wärnmark et al.[18,19] and then Gros et al.[20] increased the LF using cyclometalated Fe(II) complexes based on tridentate ligands that incorporate two n-heterocyclic carbenes. Both groups have now demonstrated efficient electron injection from related Fe(II) molecular sensitizers into TiO_2,[19,20] thus supporting the idea that MLCT excited states are not being deactivated on an ultrafast time scale. In acetonitrile (MeCN) solution phase studies of their sensitizers, where the ligands are functionalized with electron-withdrawing carboxylic acid substituents, record MLCT lifetimes of 16−18 ps are reported by both groups,[19,20] representing a 360-fold increase relative to $[Fe(bpy)_3]^{2+}$ (vide supra).[10]

We became interested in a different strategy for MLCT lifetime extension based on recent work in our group involving bis-tridentate Ru(II) systems where the terpyridyl ligands (6,6″-Br_2-2,2′:6′,2″-terpyridine) contain significant steric bulk at positions enhancing interligand repulsion.[21] We argued based on constrained density functional theory (DFT) results that these interligand interactions hinder the kinds of motions that engender coupling between the MLCT and LF manifolds.[21] However, as will be described in this current work, bis-tridentate Fe(II) complexes of the related ligand 6,6″-Cl_2-2,2′:6′,2″-terpyridine (hereafter called dctpy) do not adopt a low-spin ground-state structure. Rather, analogous to what has been seen by Constable et al. in related methyl and phenyl-substituted systems,[22] interligand repulsions push $[Fe(dctpy)_2]^{2+}$ into a quintet ground state with no evidence of singlet character at room temperature. This situation presents questions of interest to us that have not, to our knowledge, been considered in the literature. Namely, can the ^{5}MLCT manifold (which has been discussed in theoretical[23−26] and low-temperature crystal work[27]) be directly accessed from a quintet ground state, and do the structural properties within the Franck−Condon state significantly alter its subsequent nonradiative decay dynamics? Herein we argue that MLCT excitation is indeed feasible and that its lifetime, determined from our exploration of this initial system, effectively matches the longest that is known for an Fe(II) polypyridyl system.[19,20]

The dctpy ligand was synthesized using a Suzuki coupling protocol shown to be effective for similar systems,[28] wherein two chlorinated pyridyl boronic acid pinacol esters couple to a central

Received: December 28, 2015
Published: February 10, 2016

DOI: 10.1021/jacs.5b13524
J. Am. Chem. Soc. 2016, 138, 2949−2952

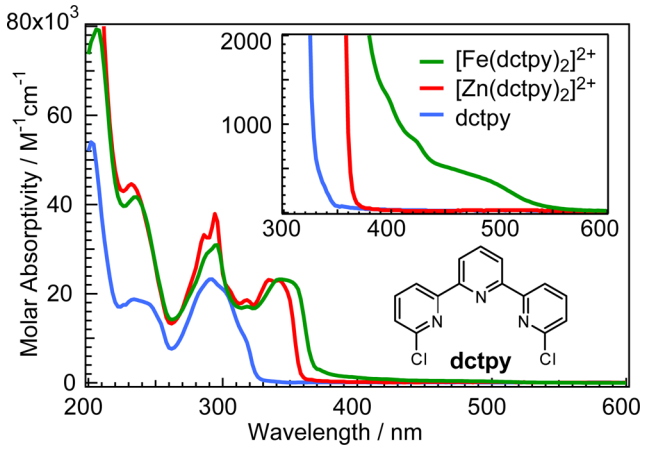

Figure 1. UV−vis absorption spectra in room-temperature MeCN of uncomplexed dctpy, $[Fe(dctpy)_2]^{2+}$, and $[Zn(dctpy)_2]^{2+}$. The inset focuses on spectral differences observed above 350 nm.

dibromopyridine to form the terpyridyl framework. The complex $[Fe(dctpy)_2]^{2+}$ was prepared under reflux conditions in 1,4-dioxane starting from the tetrafluoroborate salt of iron(II) and 2 equiv of the ligand. Weakly coordinating counterions and solvent were found to be important for avoiding competitive coordination to the metal since the steric bulk on the ligand promotes lability. A d^{10} metal complex useful for assigning electronic transitions, $[Zn(dctpy)_2]^{2+}$, was similarly prepared.

An initial indication of ground-state spin structure in $[Fe(dctpy)_2]^{2+}$ comes from room-temperature NMR experiments in acetonitrile-d_3 and the observation of ^{1}H resonances that are paramagnetically shifted between δ = 80 and −30, far beyond the normal spectroscopic region (Figure S14). Application of the Evans NMR method reveals an effective magnetic moment of 5.3 μ_B, consistent with other iron(II) species with four unpaired electrons in a distorted octahedral geometry.[22] From these measurements, and the fact that $[Fe(tpy)_2]^{2+}$ is low spin in its ground state, it is apparent that the dctpy ligand has sufficient steric bulk to weaken the LF via interligand repulsion, leading to a room-temperature quintet ground state. Although it is relatively rare, we have looked for evidence of a spin-crossover equilibrium at the temperature of our measurements. Change is neither observed in NMR spectra over the temperature range 20 to −45 °C, nor in the UV−vis spectrum of $[Fe(dctpy)_2]^{2+}$ upon cooling to −196 °C in glass-forming 2-methyl-tetrahydrofuran. For the static and time-resolved spectroscopic experiments that follow, it is clear that the dominant state subjected to photoexcitation is that of the quintet.

Molar absorptivities of dctpy and the complexes $[Zn(dctpy)_2]^{2+}$ and $[Fe(dctpy)_2]^{2+}$ have been measured in room-temperature MeCN and are shown in Figure 1. For all three species, the lowest-energy intense feature at ∼290 nm is expected to be $\pi^* \leftarrow \pi$ in nature. Upon complexation with Zn(II) or Fe(II), a second feature emerges to the red with a peak at 340 nm. Time-dependent DFT (TD-DFT) results shown in the SI nicely reproduce this observation, and natural transition orbitals (NTOs) indicate participation by both ligands (Figures S6, S10, S11). This suggests that the metal center plays a role as an electronic coupling center for ligand-to-ligand charge transfer (LLCT), excitonic splitting, or both, although spectroelectrochemical data discussed later are consistent with LLCT. A notable difference between the Fe(II) and Zn(II) species is the red-shifting of the lower energy transition and the appearance of

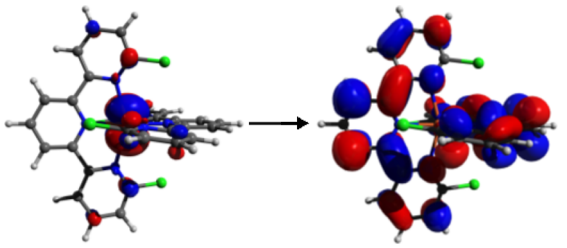

Figure 2. NTOs of $[Fe(dctpy)_2]^{2+}$ plotted for the transition (no. 11) at 410 nm. See SI for details.

Table 1. Electrochemical Data Collected in Room-Temperature MeCN vs SCE (see SI for exptl. details)

complex	$E_{1/2}$ (V)		$\Delta E_{1/2}$ [a]	ΔE_{MLCT} [b]
	3+/2+	2+/1+	(V)	(eV)
$[Fe(tpy)_2]^{2+}$	1.10	−1.26	2.36	2.2
$[Fe(dctpy)_2]^{2+}$	1.60	−0.83	2.43	∼ 3.1

[a] $\Delta E_{1/2} = E(3+/2+) - E(2+/1+)$. [b] ΔE_{MLCT}: derived from abs. spectrum in Figure 1 or for $[Fe(tpy)_2]^{2+}$.[29]

a broad absorptive feature tailing into the visible upon substitution of Zn(II) with the redox-active Fe(II) center (Figure 1 inset). In fact, we believe that this broad feature is responsible for the red-shifting of the more intense band. This feature is replicated in the TD-DFT results in the form of several low-intensity and low-energy transitions in the region from 400 to 480 nm.

While $[Fe(dctpy)_2]^{2+}$ lacks the visible extinction of its parent $[Fe(tpy)_2]^{2+}$,[29] its tailing visible feature (also seen in other high-spin systems)[7,22,30,31] with a molar absorptivity of 1200 M^{-1} cm^{-1} at 400 nm is suggestive of participation by the metal center with the possibility of MLCT originating in the quintet spin manifold, i.e., ^{5}MLCT ← ^{5}GS. While still significantly stronger than any typical LF transition, the reduced molar absorptivity of this MLCT relative to $[Fe(tpy)_2]^{2+}$ (12,000 M^{-1} cm^{-1})[29] can be rationalized since a high-spin complex will have a longer metal−ligand bond distance and less orbital overlap between the metal d and ligand π^* orbitals. We have looked for additional support of this assignment in both TD-DFT calculations and electrochemical data. In terms of the former, NTOs corresponding to the transitions in this range uniformly show β electron density on the metal relocating to the ligand, indicative of an MLCT transition (Figure 2, see also Figures S7−S9).

Considering the electrochemistry, it is noted that there is commonly a strong correlation between MLCT energies and the difference in the first one-electron oxidation and reduction potentials of coordination complexes.[32] Table 1 shows potentials measured for $[Fe(dctpy)_2]^{2+}$ and $[Fe(tpy)_2]^{2+}$ vs SCE. Focusing on the halogen-substituted molecule relative to the parent, the 2+/1+ potential undergoes a significant positive shift due to the electron-withdrawing character of the Cl atoms and their impact stabilizing unoccupied ligand π^* orbitals. At the same time, the complex becomes more difficult to oxidize, owing to two effects. First, electron density at the metal center decreases through a halogen-derived inductive effect. Second, the steric repulsions that force the high-spin state have a greater impact destabilizing the 3+ state where the LF is higher.[22] With comparable positive shifts in the 3+/2+ couple and the 2+/1+ couple, the calculated $\Delta E_{1/2}$ for $Fe(dctpy)_2]^{2+}$ is similar to that seen in $[Fe(tpy)_2]^{2+}$, thus suggesting that an MLCT state should be energetically attainable in the substituted complex.

DOI: 10.1021/jacs.5b13524
J. Am. Chem. Soc. 2016, 138, 2949−2952

One remaining question is why the MLCT transition in $[Fe(dctpy)_2]^{2+}$ appears significantly blue-shifted relative to that seen in $[Fe(tpy)_2]^{2+}$ given the observed similarity in $\Delta E_{1/2}$. A possible contributing factor has to do with metal−ligand bond lengths and the notion that a ^{1}MLCT (or ^{3}MLCT) will be stabilized more significantly than a ^{5}MLCT in terms of the coulomb interaction between the formally reduced ligand and the formally oxidized metal center. We estimate using a simple point charge model (see SI) that the ^{5}MLCT would be ∼0.7 eV higher in energy due to the larger metal−ligand bond lengths in the high-spin state, which is close to the observed difference between $\Delta E_{1/2}$ and the energy of the MLCT excitation. The reason why this is not reflected in the electrochemical experiments has to do with a difference in orbital origins of the spectroscopic vs electrochemical experiments. During the first oxidation of $[Fe(dctpy)_2]^{2+}$, the electron that is removed from the HOMO should originate from an orbital of e_g* character (using the language of an octahedral metal complex). On the other hand, the origin of the transferred charge during MLCT is t_{2g} in nature. Thus, the electrochemical estimate of the ^{5}MLCT energy (through $\Delta E_{1/2}$) will underestimate the value by an amount that is comparable to the LF splitting.

Having established the relevance of the ^{5}MLCT manifold in the visible light absorption of $[Fe(dctpy)_2]^{2+}$, we turn to spectroscopies designed to interrogate excited-state dynamics. As expected based on literature involving polypyridyl Fe(II) species, the complex is nonemissive at room temperature, suggesting that nonradiative decay channels are dominant. Therefore, TA dynamics of $[Fe(dctpy)_2]^{2+}$ have been investigated following ∼150 fs pulsed excitation at a center wavelength of 400 nm (see SI for specifications). A 2D intensity plot of TA dynamics as a function of white-light continuum probe wavelength is shown in Figure 3A with a time window of 50 ps. A number of chirp-corrected spectra from single time points are shown in the inset. As can be seen, the dominant qualitative feature from a spectral point of view is an intense near-UV absorption paired with a broad, lower intensity feature spanning the visible. A cursory view of the data set suggests some spectral evolution in the first few picoseconds and then decay to baseline of these spectral features within the 50 ps window.

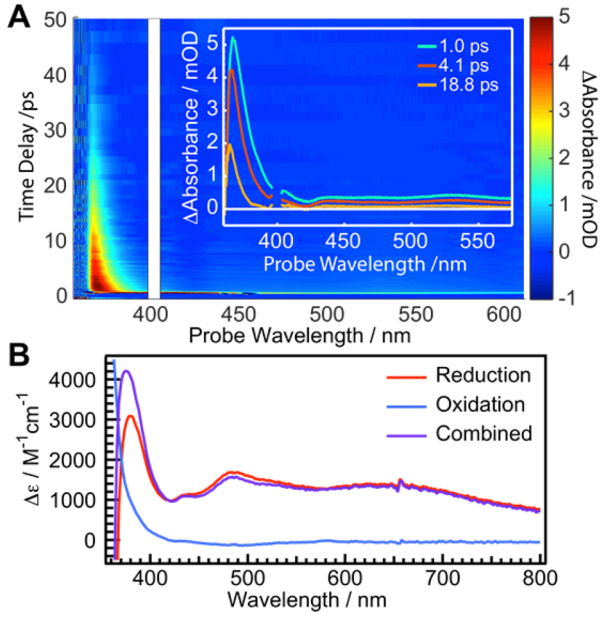

Figure 3. (A) TA spectroscopy of $[Fe(dctpy)_2]^{2+}$ in room-temperature MeCN with several individual spectra shown in the inset (pump scatter has been removed (white stripe)). (B) Quantitative spectroelectrochemical analysis of $[Fe(dctpy)_2]^{2+}$ in room-temperature MeCN based on measurement of faradaic current (see SI for details).

Before describing a quantitative analysis of the dynamics, we first consider assignment of the observed spectral features. It is possible to rule out formation of a singlet excited state (^{1}ES) with a configuration comparable to what is found in the ground state of $[Fe(tpy)_2]^{2+}$ (for simplicity: t_{2g}^6). We intuit that the steric bulk of the halogen substituents in $[Fe(dctpy)_2]^{2+}$ would prevent the development of significant visible oscillator strength in what might be a ^{1}MLCT ← ^{1}ES excitation. Further, if ^{1}ES were formed, an intense UV transition would be expected at a blue-shifted ∼340 nm akin to what is seen in $[Zn(dctpy)_2]^{2+}$, and not at 370 nm where one is actually observed. We have also ruled out the observation of a triplet LF state ^{3}MC (for simplicity: $t_{2g}^5e_g^1$). Recently such a state has been definitively observed as an intermediate in the spin-crossover dynamics of $[Fe(bpy)_3]^{2+}$.[8] Notably, however, its observation required X-ray fluorescence, as the spectral features of the ^{3}MC and ^{5}MC are too similar for distinction in ultrafast TA measurements by several groups.[7,10] Given the significant spectral differences observed in our ^{5}MC absorption (Figure 1) vs our TA (Figure 3A; inset), it is highly unlikely that the latter heralds the formation of a ^{3}MC state.

Spectroelectrochemical methods are commonly used[7,33] to identify electronic transitions relevant to MLCT states by highlighting absorptions generated due to reduction of polypyridyl systems. Using faradaic current (see details in SI) we have quantified the change in molar extinction of UV and visible features produced in $[Fe(dctpy)_2]^{2+}$ during the measurement. Upon one-electron oxidation, the principal observation is an enhancement of the ∼350 nm absorption (shown in full in Figure S1). This supports an assignment of this band to LLCT, as the intensity of such a transition would be increased through enhanced interligand electronic coupling accompanying metal oxidation and the resultant decrease of metal−ligand bond distances. Upon one-electron reduction, that same band is lost, concomitant with the growth of visible and near-UV features characteristic of the polypyridyl ligand radical anion. Superposing these redox spectra leads to a predicted difference spectrum characterized by a strong transition at ∼380 nm and a broad absorption throughout the visible. The qualitative similarity of these data with the TA difference spectra shown in the inset of Figure 3A is striking and suggests an assignment of those transient features to a MLCT excited state.

Returning to Figure 3A and focusing on Δt = 1 ps and beyond (see SI for comments about subpicosecond dynamics), the collected transient spectral data can be cleanly reproduced with a global model inclusive of only two exponential components with time constants $\tau_1 = 3.6 \pm 0.6$ ps and $\tau_2 = 16 \pm 1$ ps (error bars are 2σ for three separate data sets). Several examples of wavelength-dependent kinetics fit using this model are shown in Figure S3. To understand the components, it is first instructive to consider the time evolution of the bright UV TA feature. A comparison of normalized spectra (see Figure S4) reveals a smooth evolution of the band to a spectral position that decays with the longer time constant. In other words, there is no evidence for two distinct electronic states that interconvert on the short time scale. This indicates that 4 ps is needed for photoexcited $[Fe(dctpy)_2]^{2+}$ to thermalize within a ^{5}MLCT or ^{7}MLCT (after ultrafast intersystem crossing), including the expected inner and outer-sphere nuclear reorganization accompanying formation of a

DOI: 10.1021/jacs.5b13524
J. Am. Chem. Soc. 2016, 138, 2949−2952

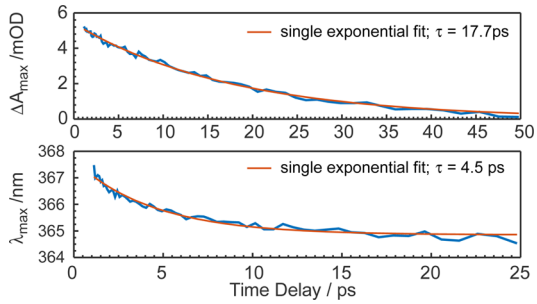

Figure 4. Shift kinetics of the 370 nm band. Top: Time evolution of the maximum Δ*A* value. Bottom: Wavelength evolution of the maximum Δ*A* as determined by a polynomial fit (e.g., Figure S4).

localized dipolar state. The second component, 16 ps, reflects the time needed for ground-state recovery with no evidence for new intermediates. It can therefore be assigned as the lifetime of the photoproduced ^{5}MLCT or ^{7}MLCT. Figure 4 (top) offers support for this assignment by showing the time evolution of the maximum TA feature in the UV. This signal decays exponentially to baseline with a time constant of 17.5 ± 1 ps, effectively matching the τ_2 value discussed above. Analysis of the time evolution of the spectral shift (4 ± 1 ps) captures the shorter time constant (Figure 4, bottom).

In summary, we have synthesized and studied a bis-dihaloterpyridine Fe(II) complex, $[Fe(dctpy)_2]^{2+}$, where inter-ligand repulsive interactions produce a high-spin quintet ground state. This complex can be excited with visible light to access the high-spin MLCT manifold where the lifetime is measured to be 16 ps or ~320-times longer than in $[Fe(bpy)_3]^{2+}$.[10] This ^{5}MLCT (or ^{7}MLCT) lifetime matches the longest that is known from low-spin ground-state systems (^{3}MCLT) where strong LFs have been exploited.[19,20] We believe this result opens new design opportunities for charge-transfer lifetime enhancement in coordination complexes of Fe(II). Next generation systems may explore whether MLCT lifetimes can be systematically tuned by variation of steric bulk, use of electron-withdrawing and -donating ligand substituents, and through intraligand electron delocalization.[33]

■ ASSOCIATED CONTENT

Supporting Information

The Supporting Information is available free of charge on the ACS Publications website at DOI: 10.1021/jacs.5b13524.

Experimental details and data (PDF)

■ AUTHOR INFORMATION

Corresponding Author

*Niels.Damrauer@colorado.edu

Author Contributions

‡These authors contributed equally.

Notes

The authors declare no competing financial interest.

■ ACKNOWLEDGMENTS

We thank Prof. M. Shores and group (CSU) for helpful discussions. The work was supported by the NSF and EPA through the Catalysis Collaboratory for Light-Activated Earth Abundant Reagents (C-CLEAR) (CHE-1339674) and utilized the Janus supercomputer (NSF; CNS-0821794).

■ REFERENCES

(1) Ardo, S.; Meyer, G. J. *Chem. Soc. Rev.* **2009**, *38*, 115.
(2) Ashford, D. L.; Gish, M. K.; Vannucci, A. K.; Brennaman, M. K.; Templeton, J. L.; Papanikolas, J. M.; Meyer, T. J. *Chem. Rev.* **2015**, *115*, 13006.
(3) Prier, C. K.; Rankic, D. A.; MacMillan, D. W. *Chem. Rev.* **2013**, *113*, 5322.
(4) Narayanam, J. M. R.; Stephenson, C. R. J. *Chem. Soc. Rev.* **2011**, *40*, 102.
(5) Yoon, T. P.; Ischay, M. A.; Du, J. *Nat. Chem.* **2010**, *2*, 527.
(6) McCusker, J. K.; Walda, K. N.; Dunn, R. C.; Simon, J. D.; Magde, D.; Hendrickson, D. N. *J. Am. Chem. Soc.* **1993**, *115*, 298.
(7) Monat, J. E.; McCusker, J. K. *J. Am. Chem. Soc.* **2000**, *122*, 4092.
(8) Zhang, W.; Alonso-Mori, R.; Bergmann, U.; Bressler, C.; Chollet, M.; Galler, A.; Gawelda, W.; Hadt, R. G.; Hartsock, R. W.; Kroll, T.; et al. *Nature* **2014**, *509*, 345.
(9) Cammarata, M.; Bertoni, R.; Lorenc, M.; Cailleau, H.; Di Matteo, S.; Mauriac, C.; Matar, S. F.; Lemke, H.; Chollet, M.; Ravy, S.; et al. *Phys. Rev. Lett.* **2014**, *113*, 227402.
(10) Aubock, G.; Chergui, M. *Nat. Chem.* **2015**, *7*, 629.
(11) Huse, N.; Cho, H.; Hong, K.; Jamula, L.; de Groot, F. M.; Kim, T. K.; McCusker, J. K.; Schoenlein, R. W. *J. Phys. Chem. Lett.* **2011**, *2*, 880.
(12) Bressler, C.; Milne, C.; Pham, V. T.; ElNahhas, A.; van der Veen, R. M.; Gawelda, W.; Johnson, S.; Beaud, P.; Grolimund, D.; Kaiser, M.; et al. *Science* **2009**, *323*, 489.
(13) Canton, S. E.; Zhang, X. Y.; Daku, L. M. L.; Smeigh, A. L.; Zhang, J. X.; Liu, Y. Z.; Wallentin, C. J.; Attenkofer, K.; Jennings, G.; Kurtz, C. A.; et al. *J. Phys. Chem. C* **2014**, *118*, 4536.
(14) Halcrow, M. A. *Chem. Soc. Rev.* **2011**, *40*, 4119.
(15) Shepherd, H. J.; Gural'skiy, I. A.; Quintero, C. M.; Tricard, S.; Salmon, L.; Molnar, G.; Bousseksou, A. *Nat. Commun.* **2013**, *4*, 2607.
(16) Jamula, L. L.; Brown, A. M.; Guo, D.; McCusker, J. K. *Inorg. Chem.* **2014**, *53*, 15.
(17) Bowman, D. N.; Bondarev, A.; Mukherjee, S.; Jakubikova, E. *Inorg. Chem.* **2015**, *54*, 8786.
(18) Liu, Y.; Harlang, T.; Canton, S. E.; Chabera, P.; Suarez-Alcantara, K.; Fleckhaus, A.; Vithanage, D. A.; Goransson, E.; Corani, A.; Lomoth, R.; et al. *Chem. Commun.* **2013**, *49*, 6412.
(19) Harlang, T. C.; Liu, Y.; Gordivska, O.; Fredin, L. A.; Ponseca, C. S., Jr.; Huang, P.; Chabera, P.; Kjaer, K. S.; Mateos, H.; Uhlig, J.; et al. *Nat. Chem.* **2015**, *7*, 883.
(20) Duchanois, T.; Etienne, T.; Cebrian, C.; Liu, L.; Monari, A.; Beley, M.; Assfeld, X.; Haacke, S.; Gros, P. C. *Eur. J. Inorg. Chem.* **2015**, *2015*, 2469.
(21) Vallett, P. J.; Damrauer, N. H. *J. Phys. Chem. A* **2013**, *117*, 6489.
(22) Constable, E. C.; Baum, G.; Bill, E.; Dyson, R.; van Eldik, R.; Fenske, D.; Kaderli, S.; Morris, D.; Neubrand, A.; Neuburger, M.; et al. *Chem. - Eur. J.* **1999**, *5*, 498.
(23) Chang, J.; Fedro, A. J.; van Veenendaal, M. *Phys. Rev. B: Condens. Matter Mater. Phys.* **2010**, *82*, 075124.
(24) De Graaf, C.; Sousa, C. *Int. J. Quantum Chem.* **2011**, *111*, 3385.
(25) Dixon, I. M.; Alary, F.; Boggio-Pasqua, M.; Heully, J.-L. *Inorg. Chem.* **2013**, *52*, 13369.
(26) Nance, J.; Bowman, D. N.; Mukherjee, S.; Kelley, C. T.; Jakubikova, E. *Inorg. Chem.* **2015**, *54*, 11259.
(27) Marino, A.; Chakraborty, P.; Servol, M.; Lorenc, M.; Collet, E.; Hauser, A. *Angew. Chem., Int. Ed.* **2014**, *53*, 3863.
(28) Voisin-Chiret, A. S.; Bouillon, A.; Burzicki, G.; Celant, M.; Legay, R.; El-Kashef, H.; Rault, S. *Tetrahedron* **2009**, *65*, 607.
(29) Braterman, P. S.; Song, J. I.; Peacock, R. D. *Inorg. Chem.* **1992**, *31*, 555.
(30) Tribollet, J.; Galle, G.; Jonusauskas, G.; Deldicque, D.; Tondusson, M.; Letard, J. F.; Freysz, E. *Chem. Phys. Lett.* **2011**, *513*, 42.
(31) Holland, J. M.; McAllister, J. A.; Kilner, C. A.; Thornton-Pett, M.; Bridgeman, A. J.; Halcrow, M. A. *J. Chem. Soc., Dalton Trans.* **2002**, 548.
(32) Lever, A. B. P. *Inorg. Chem.* **1990**, *29*, 1271.
(33) Hewitt, J. T.; Vallett, P. J.; Damrauer, N. H. *J. Phys. Chem. A* **2012**, *116*, 11536.

DOI: 10.1021/jacs.5b13524
J. Am. Chem. Soc. 2016, 138, 2949−2952